IP2016 / 4th International Workshop on Induced Polarization

Bayesian inference of spectral induced polarization parameters at the Canadian Malartic disseminated gold deposit

Charles Lafrenière-Bérubé
École Polytechnique Montréal
Address
charles.lafreniere@polymtl.ca

Michel Chouteau
École Polytechnique Montréal
Address
michel.chouteau@polymtl.ca

Gema R. Olivo
Queen's University
Address
olivo@queensu.ca

SUMMARY

Spectral induced polarization (SIP) parameters can be extracted from field or laboratory complex resistivity measurements, and even airborne or ground frequency domain electromagnetic data. There is a growing interest in application of SIP to environmental problems and mineral exploration. SIP measurements were conducted on 211 rock samples from the Canadian Malartic disseminated gold deposit to study its electric signature that could be detected by geophysical prospecting. Then, the SIP parameters were inferred using Markov-chain Monte Carlo simulation with the Cole-Cole, Dias, Debye decomposition and Shin models. Meta-sedimentary rocks with a well-defined schistosity and pyrite alteration produce higher chargeability peaks than unaltered or silicified samples. The characteristic relaxation time is also inversely related to the observable quantity of fine-grained (10^{-5} to 10^{-3} mm^2) pyrite grains per unit area. Meta-sedimentary rocks of Canadian Malartic with a pyrite content of 1 to 5% are commonly associated with gold contents above 1 ppm, and they produce a chargeability peak at short relaxation times (0.01 to 0.1 s). Unaltered rocks with fewer, larger pyrite grains (10^{-4} to 10^{-2} mm^2) produce a chargeability peak at longer relaxation times (0.1 to 10 s). Spectral induced polarization may be the key in defining the electric footprint of the Canadian Malartic and similar disseminated gold deposits, where high gold grades are associated with finely disseminated sulphides.

Key words: Spectral induced polarization (SIP), Bayesian inference, disseminated gold, quantitative mineralogy

INTRODUCTION

No specific electric or electromagnetic signature has yet been identified in the Canadian Malartic gold deposit and similar deposits. Thus geophysical prospecting for this type of deposit in similar geological environments is poorly defined. Physical properties of the ore and host rock are dependent on their mineralogical composition and textures, which relates to their original composition, deformation, metamorphism, and fluid-rock interaction history. The aim of this study is to measure the physical properties of the various rock types from the core of the mineralized system to the outer zones of the Canadian Malartic gold deposit to help anticipate the signals that could be detected by geophysical surveys. Spectral induced polarization (SIP) measurements were done on 211 core and outcrop samples from the Canadian Malartic disseminated gold deposit, in order to study its electrical footprint.

The Canadian Malartic deposit is a world class, large tonnage and low-grade Archean gold deposit located in the Pontiac Province, Québec, Canada. It is located in the proximity of the Cadillac-Larder Lake tectonic zone, south of the boundary between metamorphosed siliciclastic sedimentary rocks of the Pontiac Group and mafic to ultramafic volcanic and intrusive rocks of the Piché Group. The mineralization is hosted mainly (70%) in meta-sedimentary rocks (greywackes), partly in felsic to intermediate porphyry intrusions (monzodiorites), and rarely in mafic dykes. Gold occurs mainly as fine-grained native gold grains disseminated in the host rock, included in pyrite, or along the contacts between minerals such as pyrite, K-feldspar, plagioclase, biotite or quartz. Across the deposit, gold mineralization is associated with a halo of 1 to 5 % disseminated pyrite (Helt et al., 2014). In the 1980's, time-domain induced polarization surveys were conducted on a large part of the mining site. These surveys turned out to be inconclusive, and it is believed that the low amount (1 to 5%) of disseminated pyrite was insufficient to generate any induced polarization response.

Such small amounts of disseminated polarizable material in a porous media should generate an electrical response (Revil et al., 2015), and SIP parameters may help defining the ideal induced polarization survey parameters for prospecting similar deposits. Some ambiguity still exists in the meaning of SIP parameters such as relaxation time and chargeability. These parameters are related to the porosity and permeability of the rock (Zisser et al., 2010), and to metallic grain size and oxidation level (Gurin et al., 2013; Placiencia-Gomez et al., 2013). Several models have been proposed to fit frequency-domain induced polarization spectra and obtain these parameters. We developed an open-source Python module and standalone application to perform Bayesian inference of SIP parameters using the Debye decomposition approach, the Cole-Cole model, the Dias model, and the recently proposed model of Shin et al. (2015). Bayesian inference allows the estimation of a system's optimal parameters and their uncertainties (posterior distribution) from measurements and their errors (observations), and from knowledge about the parameters (prior distributions). The posterior distribution of SIP parameters is estimated using Markov-chain Monte Carlo (MCMC) simulation (Chen et al., 2008; Keery et al., 2012).

The SIP parameters, porosity, quantitative mineralogy, texture and whole-rock geochemistry of 12 rock samples from the Canadian Malartic gold deposit are presented. It is observed that the frequency dependence and chargeability parameters of the Cole-Cole model are related to the rocks sulfur content. Schistosity of the rock and pyrite grain orientation also

influence the SIP response, and it is noted that the quantity of metallic grain per unit area is inversely related to the relaxation time parameter of all 4 models. Experimenting with the code shows that the Cole-Cole, Debye decomposition, and Shin models converge to a solution after 1 to 5 chains of 100 000 iterations (20 to 100 seconds computation time), and often provide the best fit with experimental data. The Dias model requires only a chain of 50 000 iterations to fully converge, but we note a small discrepancy between experimental data and analytical model for most samples.

METHODS

Prior to measurements, rock samples extracted from drill cores or outcrops are drilled and cut to obtain a cylindrical core with diameter of 2.5 cm and a length of 1 to 2 cm. Samples are then wrapped in nitrile rubber and liquid paraffin is poured around the core sample in a 3.75 cm diameter by 2 cm length cylindrical mould. Once the paraffin has set, excess paraffin and nitrile rubber are removed in order to expose two opposite faces of the sample. This procedure insures that the paraffin cannot infiltrate and contaminate the rock pore network, and that all samples fit in the sample holder, where the paraffin prevents any current from circulating around the rock. Samples are then left to soak at the bottom of a tank filled with a 28 to 32 Ohm-m tap water for 48 hours.

The sample holder used for spectral induced polarization measurements is a 4-point electrodes type sample holder. Two copper needles (A-B) are used to inject current from one water-filled cell to another and two non-polarizable Ag-AgCl point-electrodes (M-N) are used to measure the voltage in the water on each side of the rock sample. The induced polarization spectra are acquired by measuring the phase shift and amplitude of complex resistivity at 17 frequencies ranging from 11.4 mHz to 750 Hz using the SIP Fuchs-III equipment from Radic Research, Germany.

One of the main advantages of using a stochastic approach to estimate the SIP parameters is that the influence of initial guesses for the parameters is decreased as the MCMC simulation progresses. This makes it ideal for batch inversion of complex resistivity spectra measured in laboratory by reducing the amount of inputs from the user. In each model we choose uniform prior distributions for the parameters to be solved. Lower and upper bounds of the prior distributions are given based on the physical meaning of the parameter (e.g. $0 <$ chargeability < 1). At each step in the chains, random values for the parameters are selected or rejected based on the Metropolis algorithm implemented in the PyMC python module. The likelihood of the corresponding simulated spectra is computed using the assumption that errors are independent for the real and imaginary parts of resistivity, and that the errors on the measurements are random and follow a normal distribution (Ghorbani et al., 2007).

RESULTS

Phase response and Debye relaxation time distribution

The textural and mineralogical attributes of two greywackes from the Canadian Malartic gold deposit are presented in Figure 1. The mineral assemblage of these two sedimentary rocks is similar, but the first one (Figure 1a) contains up to 1330 ppb Au and presents a more developed schistosity, higher pyrite content, and smaller pyrite grains (Figure 2).

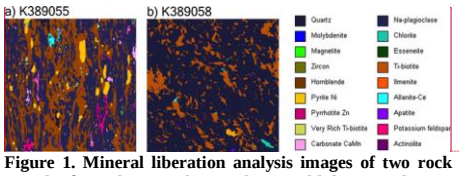

Figure 1. Mineral liberation analysis images of two rock samples from the Canadian Malartic gold deposit. The two greywacke samples, K389055 (1330 ppb Au) and K389058 (34 ppb Au), show similar mineral assemblages of quartz, plagioclase, and biotite. However, the first one displays a strong schistosity, has gold mineralization, and is altered with albite, carbonates and pyrite. Pyrite grains are aligned with the schistosity, which is marked by the preferred orientation of biotite grains.

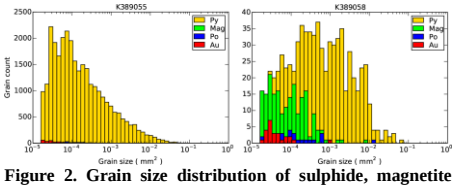

Figure 2. Grain size distribution of sulphide, magnetite and gold grains in samples K389055 (1330 ppb Au, 3.57% Py) and K389058 (34 ppb Au, 0.19% Py).

The complex resistivity spectra of both samples are also different. In the altered and foliated greywacke, the phase shift peak is observed in the 1 to 10 Hz range, while it is observed in the 0.1 to 1 Hz range for the unaltered sample (Figure 3). The high frequency response is visible on the phase spectra at frequencies above 100 Hz for the pyrite-rich rock, and frequencies above 10 Hz for the barren sample. For rock samples of similar mineral assemblage, the phase response is also higher for pyrite-rich rocks and generally lower in barren samples. Fitting the complex resistivity spectra of both rocks with the Debye decomposition approach produces the relaxation time distributions presented in Figure 4.

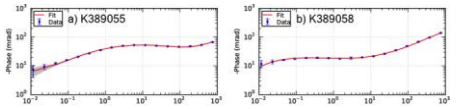

Figure 3. Phase spectra and fit with the Debye decomposition approach for rock samples (a) K389055, and (b) K389058. Both phase curves display the high-frequency response (> 100 Hz) associated with processes unrelated to the electrical double-layer. Sample K389055 displays a phase peak of -53 mrad at a frequency of 5.86 Hz and sample K389058 has a phase peak of -19 mrad at 0.37 Hz. The optimal parameters produce a response that fits the data within the measurement uncertainty in both cases.

Commenté [C1]: Will add scale (it is 1.5 mm from left to right of the square)

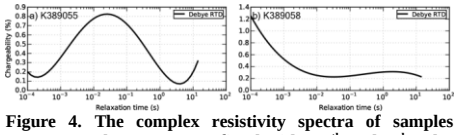

Figure 4. The complex resistivity spectra of samples K389055 and K389058 are fitted with a 4th and 3rd order polynomial Debye relaxation time distribution (RTD), respectively. The first sample has a maximum chargeability of 0.81% at a peak relaxation time of 0.02 second. The second sample has a maximum chargeability of 0.33% at a peak relaxation time of 2 seconds, when not considering the high-frequency response.

Relaxation time and pyrite grains per unit area

For all 12 samples with quantitative mineralogical information available, the characteristic relaxation time is inversely correlated to the amount of pyrite grains observed per unit area on polished thin section (Figure 5). This result is valid for the Cole-Cole, Debye, Dias and Shin models, and the relaxation times inferred using these models are correlated. It is believed that rocks with high gold contents, which are associated with a large number of small pyrite grains (Figure 2), produce a chargeability peak at shorter relaxation times than the unaltered rocks with fewer, larger pyrite grains.

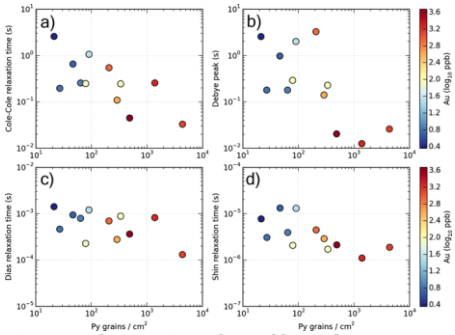

Figure 5. Relaxation times obtained by stochastic inversion on 12 rock samples from the Canadian Malartic gold deposit. The gold content of each sample is shown by the colour legend bar. In the Cole-Cole model, rock samples with over 1000 ppb Au tend to possess a characteristic relaxation time that is lower than 0.1 second. The same observation is made when using the Debye decomposition approach and considering the peak relaxation time in the RTD.

SIP parameters, physical properties and sulphide content

Considering all 211 samples, no direct link was found between chargeability and sulphide content using the four SIP models. However, we noted that the chargeability (m) and frequency dependence (c) parameters are correlated in the Cole-Cole model. Consequently, as the MCMC simulation progresses, small increments in chargeability in the range (0.2-0.3) are compensated by small decrements in frequency dependence in the same range. One way to remove this correlation is to fix the frequency dependence to a value of 0.25. Fixing frequency dependence, however, significantly reduces the quality of the fit. Another way is to consider a combination of both parameters (e.g. c + m). Using this combination, we find that both frequency dependence and chargeability are related to total sulphur content determined by X-Ray Fluorescence method (Figure 6). Values for porosity, resistivity, magnetic susceptibility, density, chargeability, relaxation time, and pyrite content are presented in Table 1. The relaxation time values are strongly correlated from one model to another, but only the Dias, Debye, and Shin chargeabilties are correlated together. The Cole-Cole chargeability is only correlated with the three other models when the frequency dependence parameter is fixed.

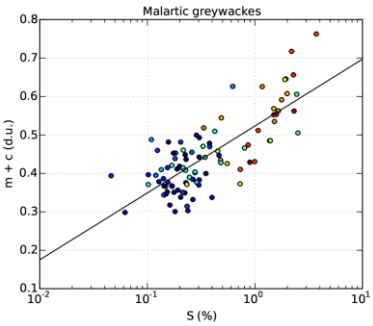

Figure 6. Correlation between sulphur content and the addition of chargeability (m) and frequency dependence (c) parameters of the Cole-Cole model (r = 0.636).

Commenté [C2]: The color is representative of gold content. Will update the figure for the colors to match Figure 5 and add legend.

CONCLUSIONS

Previous time-domain induced polarization work has failed to identify any chargeability or resistivity anomalies at the Canadian Malartic gold deposit. However, the analysis of rock complex resistivity spectra measured in the laboratory shows that pyritic alteration in high-schistosity sedimentary rocks produces chargeability peaks at shorter relaxation times than unaltered rocks. Contrary to what might be expected, no direct link between chargeability and pyrite content is observed. However, the chargeability and frequency dependence parameters are correlated and are both related to total sulphur content. In fact, some of the most altered and pyrite-rich samples are also silicified, which could fill the pore connectivity, reduce porosity and therefore attenuate the SIP response. The results presented here are in agreement with the principle that smaller polarizable particles are associated with shorter relaxation times (Gurin et al., 2013). Spectral induced polarization may be the key in defining the electric footprint of the Canadian Malartic and similar disseminated gold deposits. When gold is present as inclusions in microscopic pyrite grains, the induced polarization response is maximal between frequencies of 1 to 10 Hz. In the near future, more SIP measurements and stochastic inversions will be conducted on a more extensive collection of samples from the Canadian Malartic gold deposit, the Highland Valley porphyry-copper deposit, and the Millennium-McArthur uranium deposits to test the model.

ACKNOWLEDGMENTS

Thanks to S. Perrouty, N. Gaillard, P. Lypaczewski, N. Blacklock, T. Raskevicius, R. Mir, R. Thiémonge, and G. Gauthier for helping with sampling and fieldwork. Research funded by Canada Mining Innovation Council (CMIC) and NSERC CRD Program. CMIC-NSERC Exploration Footprints Network Contribution 093.

REFERENCES

Chen, J., Kemna, A., and Hubbard, S. S. (2008). A comparison between Gauss-Newton and Markov-chain Monte Carlo–based methods for inverting spectral induced-polarization data for Cole-Cole parameters. Geophysics, 73(6): F247–F259.

Ghorbani, A., Camerlynck, C., Florsch, N., Cosenza, P., and Revil, A. (2007). Bayesian inference of the Cole–Cole parameters from time- and frequency-domain induced polarization. Geophysical Prospecting, 55(4): 589–605.

Gurin, G., Tarasov, A., Ilyin, Y., and Titov, K. (2013). Time domain spectral induced polarization of disseminated electronic conductors : Laboratory data analysis through the Debye decomposition approach. Journal of Applied Geophysics, 98: 44–53.

Keery, J., Binley, A., Elshenawy, A., and Clifford, J. (2012). Markov-chain Monte Carlo estimation of distributed Debye relaxations in spectral induced polarization. Geophysics, 77(2): E159–E170.

Placencia-Gomez, E., Slater, L., Ntarlagiannis, D., and Binley, A. (2013). Laboratory SIP signatures associated with oxidation of disseminated metal sulfides. Journal of Contaminant Hydrology, 148: 25–38.

Revil, A., Florsch, N. and Mao, D. (2015). Induced Polarization Response of Porous Media with Metallic Particles — Part 1: A Theory for Disseminated Semiconductors. Geophysics, 80(5): D525–38.

Shin, S. W., Park, S., and Shin, D. B. (2015). Development of a New Equivalent Circuit Model for Spectral Induced Polarization Data Analysis of Ore Samples. Environmental Earth Sciences 74(7): 5711–16.

Zisser, N., Kemna, A., and Nover, G. (2010). Relationship between low-frequency electrical properties and hydraulic permeability of low-permeability sandstones. Geophysics, 75(3): E131–E141.

Sample ID	Au (ppb)	Py (%)	Mag susc (SI)	Density (g/cc)	Porosity (%)	Resistivity (Ohm-m)	ColeCole m	ColeCole tau (s)	ColeCole c	Debye m	Debye Peak (s)	Dias m	Dias tau (s)	Shin m	Shin tau (s)
K389005	395	0.95	2.94E-04	2.767	0.161	5.37E+03	0.102	1.09E-01	0.407	0.112	1.41E-01	0.151	2.77E-04	0.098	2.88E-06
K389019	1840	2.73	1.22E-04	2.759	0.296	5.35E+03	0.027	2.56E-01	0.630	0.251	1.26E-02	0.253	8.20E-04	0.169	1.10E-06
K389046	5.2	0.17	4.50E-05	2.751	0.092	1.22E+04	0.145	6.53E-01	0.505	0.304	9.74E-01	0.322	9.38E-04	0.216	1.32E-05
K389055	1330	3.57	2.19E-04	2.827	0.259	4.90E+03	0.197	3.29E-02	0.537	0.216	2.60E-02	0.323	1.31E-04	0.199	1.88E-06
K389058	34	0.19	4.83E-04	2.743	0.03	6.01E+03	0.111	1.06E+00	0.369	0.203	2.01E+00	0.268	1.20E-03	0.193	1.30E-05
K389062	7.4	0.35	1.98E-02	2.762	0.14	5.03E+03	0.098	2.56E-01	0.422	0.199	1.79E-01	0.211	7.92E-04	0.169	3.92E-06
K389077	2.3	0.01	1.34E-03	3.066	0.219	2.97E+04	0.057	2.58E+00	0.318	0.088	2.56E+00	0.156	1.41E-03	0.113	7.70E-06
K389198	93.1	0.70	7.50E-05	2.703	0.288	8.97E+03	0.052	2.45E-01	0.471	0.137	2.28E-01	0.148	8.80E-04	0.114	1.71E-06
K389214	6.3	0.22	2.71E-04	2.735	0.118	9.30E+04	0.114	1.96E-01	0.540	0.227	1.79E-01	0.246	4.63E-04	0.186	3.06E-06
K389216	833	0.35	4.22E-04	2.762	0.117	2.34E+04	0.065	5.44E-01	0.268	0.067	3.26E+00	0.132	6.95E-04	0.064	4.45E-06
K389219	4720	1.79	2.54E-04	2.776	0.156	8.00E+03	0.079	4.48E-02	0.311	0.072	2.04E-02	0.113	3.62E-04	0.084	2.12E-06
K389227	87.8	1.26	7.83E-03	2.711	0.205	1.31E+04	0.156	2.48E-01	0.461	0.181	2.91E-01	0.215	2.27E-04	0.151	2.07E-06

Table 1. Gold and pyrite contents, magnetic susceptibility, density, porosity, resistivity and spectral induced polarization parameters of 12 rock samples from the Canadian Malartic gold deposit.